Efficient photocatalytic water splitting using Sn-doped $SrTiO_3$ perovskite with Sn at Sr sites

Yongshuai Chen [a], Mengdie Cai [a *], Yimeng Cao [a], Suhaib Shuaib Adam Shuaib [a], Jia-qi Bai [a *], Fang Chen [a], Jiawei Xue [b], Yuxue Wei [a] and Song Sun [a]

[a] *School of Chemistry and Chemical Engineering, Anhui University, Hefei, Anhui 230601, China*

[b] *National Synchrotron Radiation Laboratory, University of Science and Technology of China, Hefei, Anhui, 230029, China*

Corresponding authors: Jia-qi Bai (jiaqibai@ahu.edu.cn); Mengdei Cai (caimengdie1987@163.com)

Computational Methods and Details.

The adsorption energy (ΔE_{ads}) of H_2O on the (100) surface of $SrTiO_3$ and Sn doped $SrTiO_3$ was calculated using the following equation:

$$\Delta E_{ads} = E_{slab\text{-}H_2O} - (E_{slab} + E_{H_2O}) \quad \text{Eq.(S1)}$$

where $E_{slab\text{-}H_2O}$ represents the total energy for the adsorption state, E_{slab} represents the energy of the clean catalyst surface, and E_{H_2O} represents the energy of a H_2O molecular. A more negative value of ΔE_{ads} indicated higher stable adsorption system. Surface redox reactions are a crucial element in the photocatalytic water splitting process.

The doping sites and doping stability were evaluated through formation energy calculations. The formation energy (E_f) is defined as:

$$E_f = E_{doped} - E_{undoped} + n\mu_i - n\mu_j \quad \text{Eq.(S2)}$$

where E_{doped} and $E_{undoped}$ represent the total energies of the doped and pristine supercells, respectively, n denotes the number of atoms removed or added, and μ_i and μ_j represent the chemical potentials of removing and adding atoms, respectively. To maintain chemical potential equilibrium with bulk phases, the chemical potentials of metallic Sr, Ti, and Sn were derived from the energy per atom in their corresponding bulk materials.

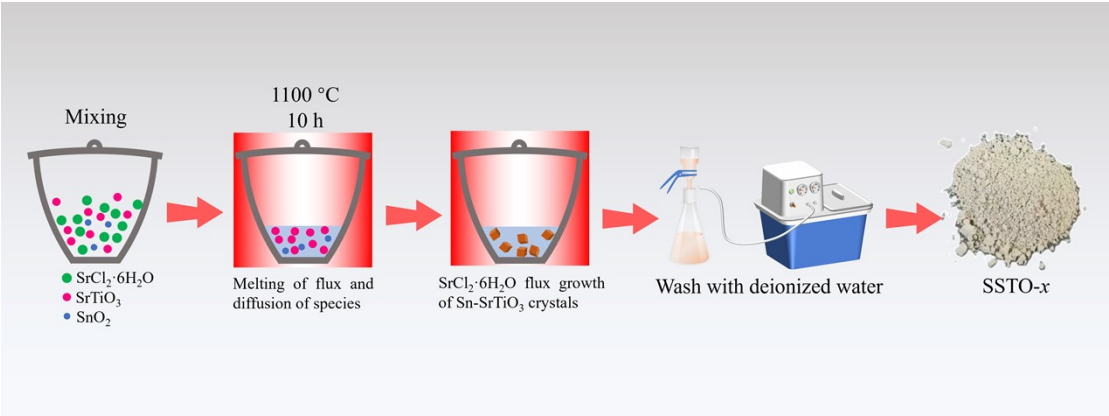

Scheme. 1. Schematic illustration of the fabrication process of SSTO-*x* samples.

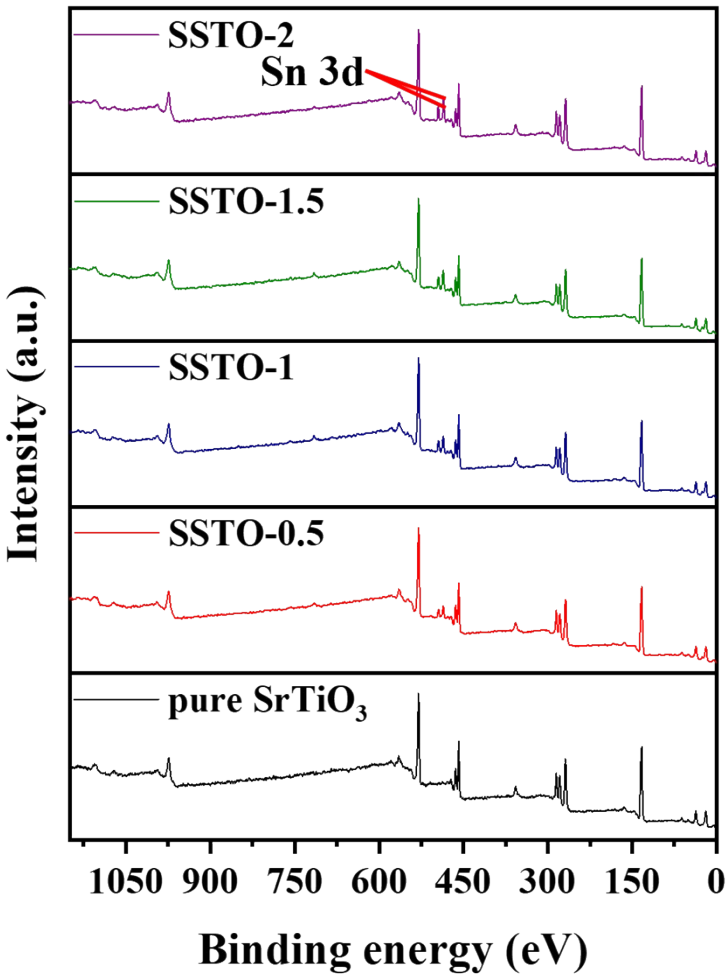

Fig. S1 Survey XPS spectra of the as-prepared catalysts.

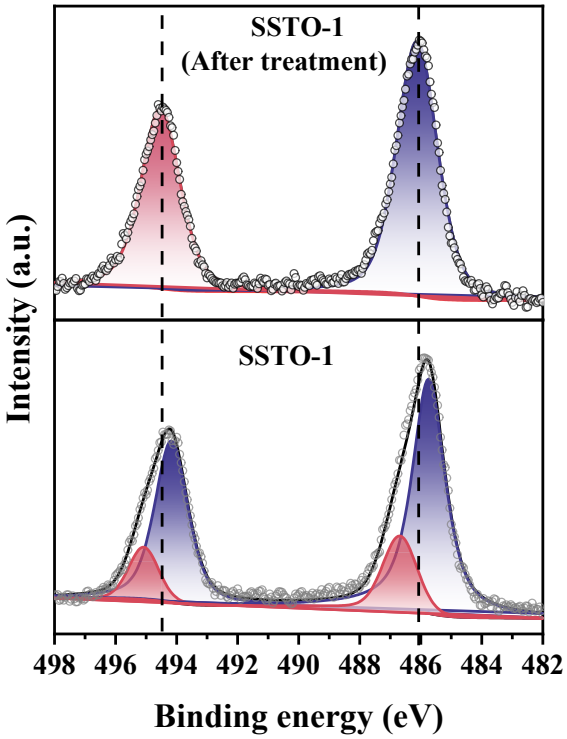

Fig. S2 High-resolution Sn 3d X-ray photoelectron spectroscopy before and after alkaline treatment of SSTO-1 samples.

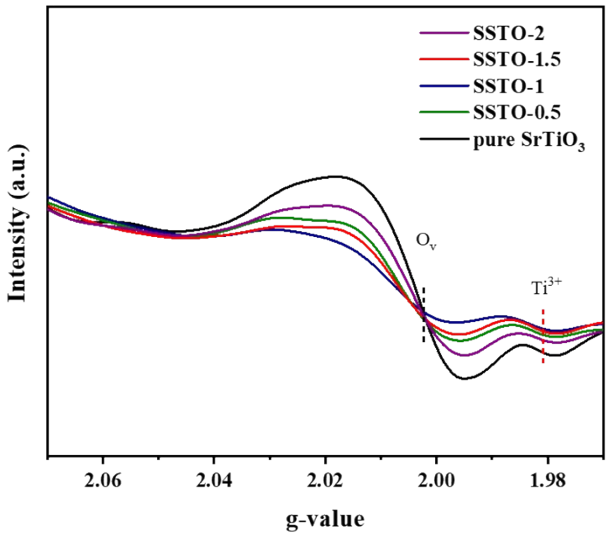

Fig. S3 Electron paramagnetic resonance spectra of the as-prepared catalysts.

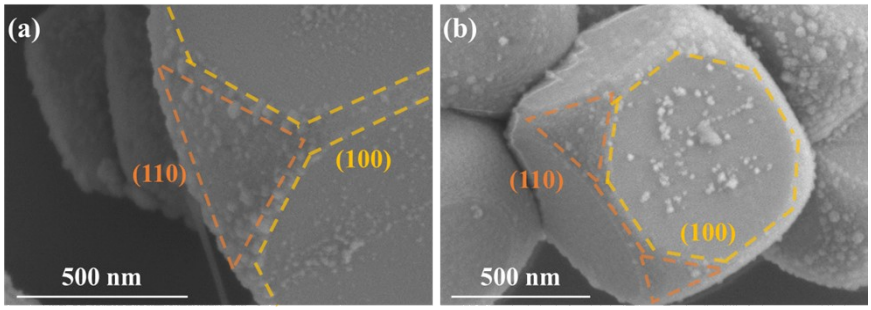

Fig. S4 (a-b) SEM images of the SSTO-1 samples after the deposition of the cocatalysts.

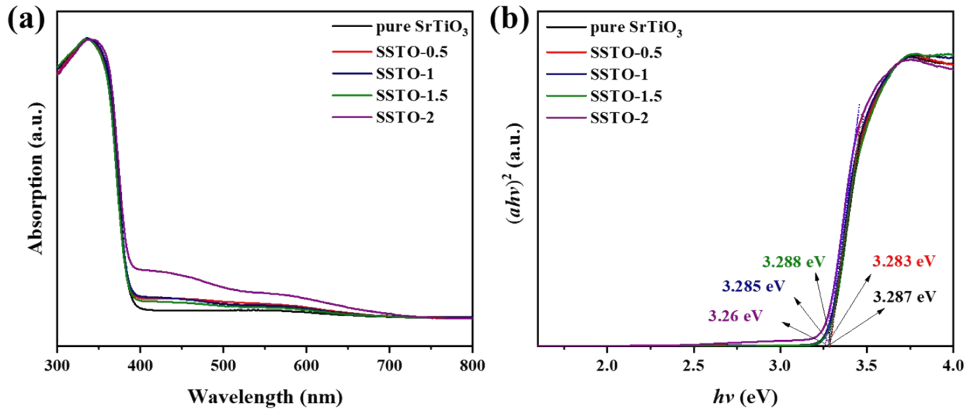

Fig. S5 (a) UV-vis DRS and (b) Plots of $(ahv)^2$ vs. (hv) of the as-prepared catalysts.

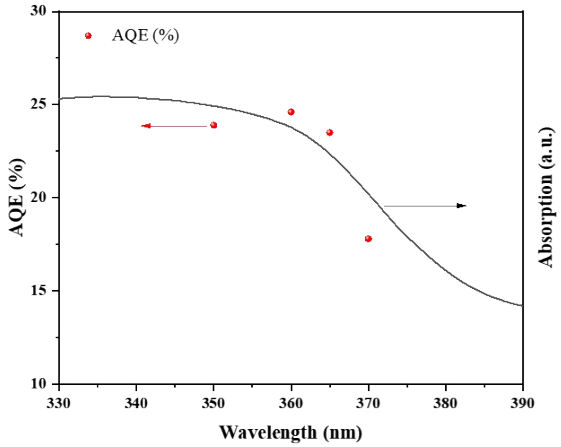

Fig. S6 The wavelength dependence of the apparent quantum efficiency (AQE) of the SSTO-1 sample in the water splitting reaction.

Table. S1 Composition and content of Sr^{2+} species on the surface of the as-prepared catalyst.

Sample	Area		R_1
	Perovskite Sr	Suboxide	
pure $SrTiO_3$	24746.11	13872.778	1.78
SSTO-0.5	63851.44	38289.61	1.67
SSTO-1	63244.93	38571.7	1.64
SSTO-1.5	58308.71	38919.87	1.5
SSTO-2	53786.64	38426.6	1.40

Table. S2 Composition and content of Ti species on the surface of the as-prepared catalyst.

Sample	Area		R_2
	Ti^{4+}	Ti^{3+}	
pure $SrTiO_3$	20719.924	15128.074	1.37
SSTO-0.5	58454.82	40242.27	1.45
SSTO-1	58005.81	37242.06	1.56
SSTO-1.5	55105.28	36040.23	1.53
SSTO-2	48927.32	36193.23	1.35

Table. S3 Composition and content of O species on the surface of the as-prepared catalyst.

Sample	Area		R_3
	O_{lat}	O_{ads}	
pure $SrTiO_3$	36600.41	13310	2.75
SSTO-0.5	101459	40799.31	2.49
SSTO-1	100724.2	43168.21	2.33
SSTO-1.5	100020.3	42596.96	2.35
SSTO-2	91887.89	37239.25	2.47

Table. S4 The experimental data required for the apparent quantum efficiency test.

Wavelength (nm)	**Irradiation intensity (mW/cm^2)**	**H_2 evolution ($\mu mol \cdot h^{-1}$)**	**A (cm^2)**	**E_g (eV)**	**AQE (%)**
350	10.54	53.27	4	3.543	23.9
360	10.72	57.28	4	3.444	24.6
365	10.22	52.76	4	3.397	23.5
370	9.21	36.57	4	3.351	17.8

Table. S5 The adsorption energy of H_2O molecules on the (100) surfaces of pure $SrTiO_3$ (100) and Sn doped $SrTiO_3$(SSTO).

Energy/eV	E_{H_2O}/eV	$E_{(100)}$/eV	$E_{(100)\text{-}H_2O}$/eV	ΔE_{ads}/eV
pure $SrTiO_3$	-471.89	-80182.01	-80654.74	-0.84
SSTO	-471.89	-81361.14	-81834.18	-1.15